RESEARCH ARTICLE OPEN ACCESS

A Novel Approach to Analyze Satellite Images for Severe Weather Events

Shreyas Fadnavis
Pune Institute of Computer Technology, Pune, India

ABSTRACT
Severe weather events (e.g. cyclones, thunderstorms, fog, floods etc.) have catastrophic effects on human life and aggrandize the impacts on agriculture, economy etc. Therefore information related to severe weather, in any form, is important for mitigation purposes and helps in delineating the causes and influences responsible. Satellites images provide such information related to the formation of such events at early stages and help in tracking its spatial and temporal development. This paper presents a framework to obtain maximum information of severe weather events from satellite panoramas. The backbone of this proposed framework involves high quality filtering of noise followed by a region growing technique which seeds each pixel, thus providing refined information for further extraction. This approach will be very helpful not only for acquiring valuable information of developing severe weather events, but also for other fields (e.g. medical and astronomy) where high precision imaging is required.
Keywords: Satellite Images; Cyclone; Double Wiener Filter; Block Adaptive Window.

I. Introduction

Satellite images have applications in variety of fields e.g. meteorology, oceanography, fishing, agriculture, biodiversity conservation, forestry, landscape, astronomy, geology etc [1,2,3.4]. Satellite provides high resolution imageries which help in the retrieval of information regarding the development of severe weather events in any part of the globe. Cyclone is one such severe weather event which has catastrophic effects on human life [2]. The analysis of such satellite imaginaries helps to provide prompt and valuable information of such events at early stages of its formation. It therefore helps the forecasters and in turn for mitigation purposes. The onboard sensors of satellites and weather conditions can affect image quality to a certain degree [5]. These images are also degraded by noise during the acquisition and transmission processes [6]. Satellite images have inherent speckle, striping or coherent noise which is produced because of the variation in backscatter from inhomogeneous cells [7]. Coherent Noise (CN) appears as a repeating pattern in satellite imagery [8]. It is essential to de-noise the satellite images and extract valuable information from the developing server weather systems in order to reduce its impact on human life. In the following sections we discuss a new method to obtain maximum information from satellite images. We examine the effectiveness of this algorithm on a satellite panorama of a cyclone image.

II. De-noising algorithm

The wavelet transform is an efficient tool for signal analysis in the time–frequency domain. It is a very effective in filtering the transient signals [9]. We apply block adaptive windows in local doubly Wiener filtering [10, 11] to improve the image's energy distribution. In this section a brief description of doubly local wiener filtering scheme is presented [10, 12]. In the wavelet domain, the wavelet coefficients of observed noisy image are represented as

$$W_{k,l}(i,j) = S_{k,l}(i,j) + \varepsilon_{k,l}(i,j), \quad i,j = 1,2,3,\ldots..N \qquad (1)$$

Where, k and l represent the scales and oriented sub-bands respectively. $S_{k,l}$ and $\varepsilon_{k,l}$ are the wavelet coefficients of noise free image and noise respectively. $W_{k,l}$ is total wavelet coefficient. The term $\varepsilon_{k,l}(i,j)$ is zero mean Gaussian random variable of variance $\sigma^2_{k,l}(i,j)$. The noise variance distribution $\sigma^2_{k,l}(i,j)$ of sub-images is calculated from $\sigma^2(i,j)$ by the energy filter bank [10]. Let {h,g} are an orthonormal filter bank for decomposition. The Corresponding equivalent filter bank

The filer bank in 2-D tensor wavelet is written as:

$$H^e_{0,l}(z_1,z_2) = H^e_l(z_1)\, H^e_l(z_2) \quad H^e_{1,l}(z_1,z_2) = G^e_l(z_1)\, H^e_l(z_2)$$
$$H^e_{2,l}(z_1,z_2) = H^e_l(z_1)\, G^e_l(z_2) \quad H^e_{3,l}(z_1,z_2) = G^e_l(z_1)\, G^e_l(z_2) \qquad (2)$$

Where k denotes the oriented sub-band and l denotes the level of the decomposition. The noise variance distributions in the sub-images are calculated as [13]

$$\sigma^2_{k,l}(i,j) = \sum_m \sum_n [h^e_{k,l}(m,n)\ \sigma^2(i-m, j-n) \quad (3)$$

The filter bank $[h^e_{k,l}(m,n)]^2$ corresponds to the energy filter bank of the 2-D wavelet. In double local Wiener filtering, the second Wiener filtering is used to improve denoising by improving energy distribution. The flowchart of double local Wiener filtering algorithm [13] can be given as:

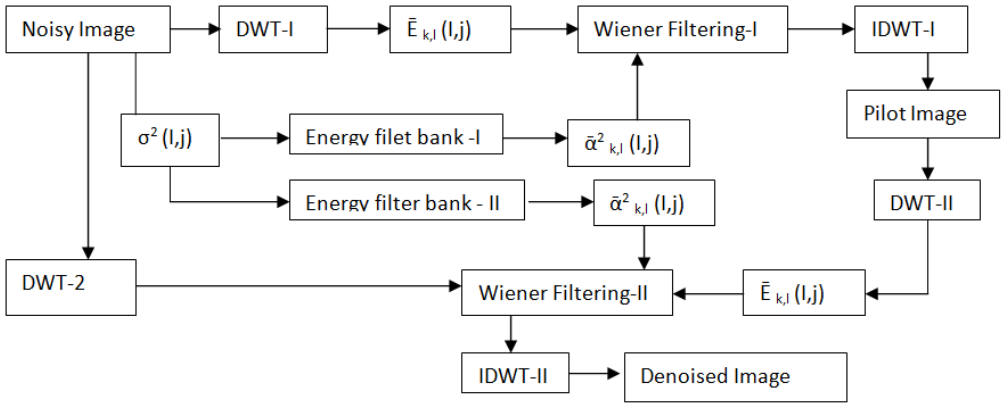

Figure 1. Flow chart of double Wiener filtering algorithm.

The estimation of energy distribution is related to the final denoising performance [10]. The performance of estimators depends on the sizes and shapes of the windows. To improve energy distribution of an observed image we used block-adaptive window.

III. The Block-Adaptive windows

It is known that in an observed image the energy clusters are distributed along the spatial direction (principal direction) in most of the data blocks [14]. The energy distribution estimate of an image using a fixed window is blurred in some regions where direction of a window and energy clusters is oriented in different directions. Figure 2 exhibits energy distributions of horizontal, vertical and diagonal sub- bands and their block energy correlation function.

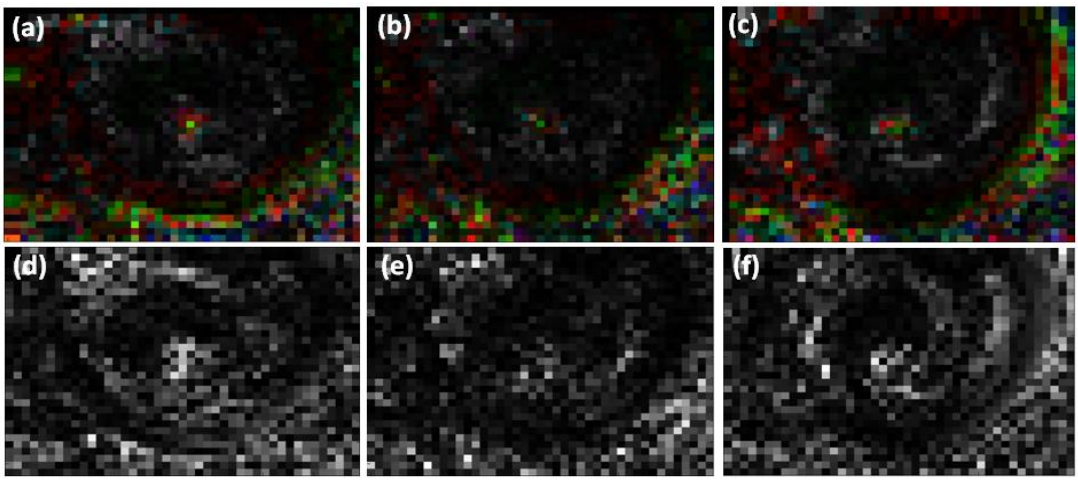

C

Figure 2: the energy distribution of the satellite image of a cyclone at the second level and their block energy correlation function applied on the noisy image. Noisy image is generated by adding Gaussian noise of σ=10.

One can see that energy clusters are distributed along principal direction of data block. Therefore use of fixed square or elliptic directional windows may cause a mismatch with the directions

of energy clusters and may cause blurring of an image. Figure 3 (a) shows the true energy distribution of the original image, and figures 3 (b) – (d) show energy distributions using square, elliptical and block adaptive windowing. These figures show that energy clusters are distributed along the principle direction of a data block. Therefore blurring of an image can be reduced by adjusting the direction of the window in its principle direction. We used the BECOF of data block of 5th order of wavelet coefficient and then a block adaptive directional window was applied on it. The block energy correlation function is given as:

$$\text{BECOF}_{m,n}(p,q) = \sum_{i=0}^{2^{h-1}} \sum_{j=0}^{2^{h-1}} \check{s}^2(2^{j1}m + i, 2^{j1}n + j)\check{s}^2(2^{j1}m + i + p, 2^{j1}n + j + q) \quad (4)$$

The estimation of energy distribution is obtained as

$$\check{s}^2(i,j) = \max\{0, w)\, i,j) - \sigma^2(i,j) \quad (5)$$

Where σ^2 (i,j) is its noise variance distribution.
Therefore, we propose to use the block covariance matrices of wavelet coefficients to improve the performance of the Wiener filtering [10]. For a given window size is Q, we select the shape of the window for every block, as per its block energy correlation (BECOF) function by:

$N_1(m,n) = \{(p,q):\text{BECOF}_{m,n}(p,q) \geq \Upsilon$ (6)

Υ is the Qth largest entry of matrix block adaptive correlation function.

The image energy distribution in a subimage for the first Wiener filtering is block-wise estimated As

$$\bar{E}(I,j) = \max\{0, \frac{1}{\#N1(m,n)} \sum_{(p,q)\in N1(m,n)} w_i^2(i+p,j+q) - \sigma_i^2(i+p,j+q))\} \quad (7)$$

M=floor(2^{-j}, i), n=floor (2^{-j},j)
Where the floor(x) rounds x to the nearest integer towards minus infinity.
As can been seen from Figures 3 (a) – 3(d) square and elliptical windows blurred estimates while block adaptive window gives better estimates since the shape of the window matches with the principal direction of the energy cluster.

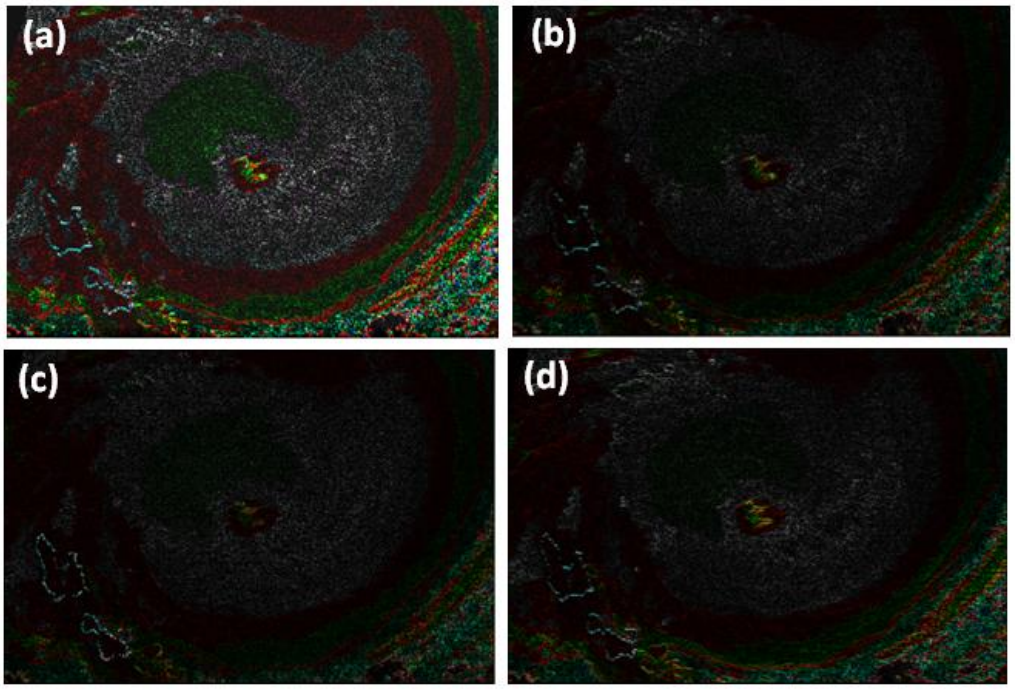

Figure 3 The energy distribution of (a) Satellite image (b) energy distribution by (c) square (d) elliptical and (d) block adaptive windows of vertical sub images at level 5 of noise with σ =10.

During the application of second Wiener filtering, block energy correlation function and noise variance are assumed to be zero. The windows of smaller size are obtained as per equation (4) and energy distributions are re-estimated as (5). For efficient computations, we use FFT to compute block adaptive correlation coefficient for multiple times of multiplications. In figure 4 (a) -4(c) we show denoised

image in horizontal, vertical and diagonal oriented sub-bands and corresponding details are shown in histograms (see figures 4 (d)-(e)).

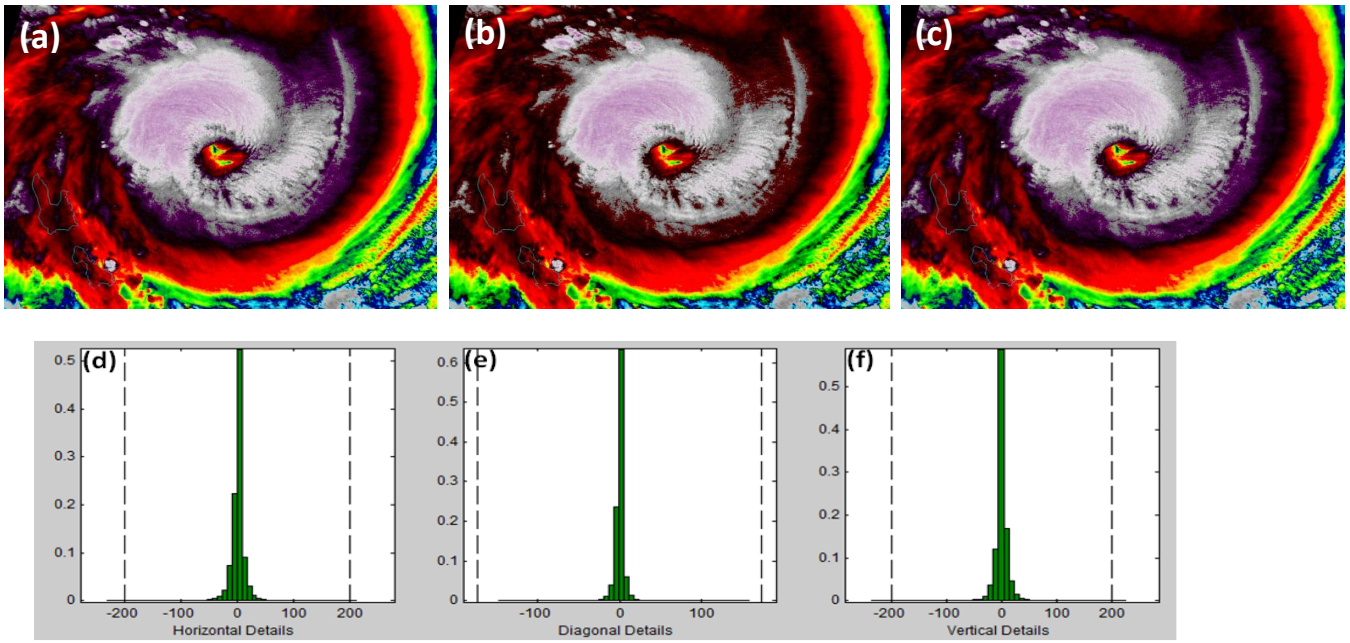

Figure 4: Denoised image in (a) horizontal, (b) vertical and (c) diagonal oriented sub-bands and corresponding details are shown in (e), (f) and (g) histograms.

IV. Region Growing

Satellite weather maps are highly textured with a variation in their intensities across the image. These images provide information to indicate that the weather may turn to severe weather conditions in near future. In order to retain this valuable information and to improve the retrievable energy, we apply an algorithm for segmentation of the intensity image. This is applied on the denoised image obtained after application block adaptive windows in local double Wiener filter in order to eliminate noise distribution in the pixel. Region growing is done by examining properties of each block and merging them with adjacent blocks that satisfy some criteria. We used a criterion that looks at the max-min difference and combines the adjacent regions whose max-min difference is within the tolerance of the seed block [15, 16]. The new region is now the seed and the process is repeated, examining adjacent regions, comparing max-min differences and adding blocks that are within the tolerance specified by the user. This tolerance does not have to be the same as the threshold used in the merge-split algorithm. Alternatively, the mean values of the blocks can be used to determine which blocks should be merged. Figure 5 (a) is a noisy satellite image of a cyclone and figure 5 (b) is an improved image obtained after application of region growing algorithm. It is quite evident the image obtained after application of proposed framework i.e. high quality filter application of block adaptive window using double local filtering followed by region growing by seeding pixels, reduces spatial non stationary noise in the image.

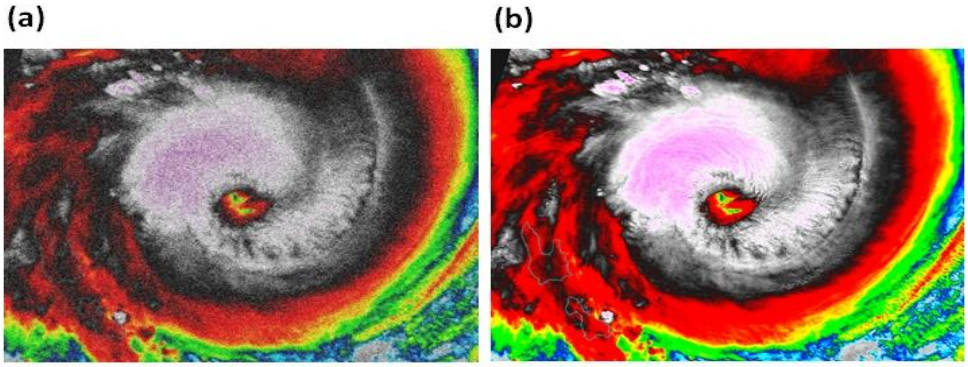

Figure 5: (a) Satellite image of cyclone with additive white Gaussian noise at σ = 10 (b) an image obtained after application of region growing on denoised image.

V. Conclusions

Severe weather events such as cyclones have serious implications and can use serous damages to human life. Satellite panoramas give information of its formation at early stages. In this paper we propose an algorithm to optimize such information obtained from satellite panoramas for mitigation purpose. We proposed an algorithm containing a submodule of double Wiener filter with block adaptive window to denoise satellite panoramas by taking into account energy distribution. We also proposed to use another submodule of region growing to maximize the information of severe weather (e.g. cyclone) satellite panoramas. It is done by examining properties of each block and merging them with adjacent blocks that satisfy some criteria. We used a criterion to calculate the difference between maximum and minimum (max-min) and combine adjacent regions whose max-min difference is within a tolerance of the seed's blocks. The new region is now the seed and the process is repeated, examining adjacent regions, comparing max-min differences, and adding blocks that are within the tolerance specified by the user. The results show that high quality filtering using double Wiener filter with block adaptive window effectively reduces additive white Gaussian noise. The denoised image is then grown to maximize the information to be extracted.

Acknowledgement

The author acknowledges the facilities provided by the college staff and library at Pune Institute of Computer Technology which were very helpful.

References:

[1] Liao D-Y, Yang Y-T: 'Satellite imaging order scheduling with stochastic weather condition forecast Systems', Man and Cybernetics, IEEE International Conference on Oct. 2005, 3, pp 2524 – 2529.

[2] Wasimi, S.A., Saha, K.K.: 'An expert system to assess the landfall propensity of a tropical cyclone in Australia', Computer Science and Engineering (APWC on CSE), Asia-Pacific World Congress on , Nov. 2014, pp.1-6 .

[3] Zhenzhou P. Shinjae Y., Yu D.; Huang D.: 'Solar irradiance forecast system based on geostationary satellite', Smart Grid Communications (SmartGridComm), IEEE International Conference on, Oct. 2013, pp. 708 - 713.

[4] Yi P., Zhao Y., '3D landscape development based on the high-resolution satellite image', Remote Sensing, Environment and Transportation Engineering (RSETE), International Conference on, June 2011, pp. 8011 - 8014 .

[5] Ravinder, A. Reddy, P.K. ; Prasad, N.: 'Detection of Wavelengths for Hail Identification Using Satellite Imagery of Clouds', Computational Intelligence, Communication Systems and Networks (CICSyN), Fifth International Conference on, June 2013, pp. 205 - 211.

[6] Huang, X., Madoc, A.C., Cheetham, A.D., 'Multi-noise removal from images by wavelet-based Bayesian estimator', Multimedia Software Engineering, Proceedings. IEEE Sixth International Symposium on, December. 2004, pp. 258 - 264.

[7] Hu C., Feng L., Lee Z., Davis C. O., Mannino A., McClain C. R., Franz B. A,: 'Dynamic range and sensitivity requirements of satellite ocean color sensors: learning from the past', Applied Optics, 2012, 51(25), pp. 6045-6062.

[8] Aiazzi, B., Alparone, L., Baronti, S., Garzelli, A.: 'Coherence estimation from multilook incoherent SAR imagery', Geoscience and Remote Sensing, IEEE Transactions on, 2003 41(11), pp. 2531 - 2539 .

[9] Fang H-T., Huang D-S.: 'Noise reduction in lidar signal based on discrete wavelet transform', Optics Communications, 2004, 233(1), pp. 67–76.

[10] Peng-lang Shui and Yong-Bo Zhao, Image denoising algorithm using doubly local Wiener filtering with block-adaptive windows in wavelet domain, Signal Processing, 2007, 87(7), PP.1721-1734.

[11] Li D., Yan W.; Ting F.: 'Wavelet image denoising algorithm based on local adaptive wiener filtering', Mechatronic Science, Electric Engineering and Computer (MEC), International Conference on, August 2011, pp. 2305 - 2307.

[12] Shui P-L: "Image denoising algorithm via doubly local Wiener filtering with directional windows in wavelet domain," IEEE Signal Processing Letters, 2005, 12(10), pp. 681-684.

[13] Argenti F., Alparone L.,: 'Speckle removal from SAR images in undecimated wavelet domain,' IEEE Trans. Geosci. Remote Sensing, 2002, 40(11), pp.2363-2374.

[14] Zhong, S. ; Cherkassky, V.: 'Image Denoising using Wavelet Thresholding and Model Selection' Image Processing 2000, Proceedings. 2000 International Conference on, 3, Sept. 2000, pp. 262 – 265.

[15] Huang A., Li J., Summers R. M., Petrick N., and Hara A. K.,: 'Improving Polyp Detection Algorithms for CT Colonography:

Pareto Front Approach', Pattern Recognit Lett. 2010, 31(11), pp. 1461–1469, doi: 10.1016/j.patrec.2010.03.013.

[16] Wee L.K., Chai H. Y. and Supriyanto E.: 'Three dimensional nuchal translucency ultrasoundsegmentation using region growing for trisomy 21 early assessment'. International Journal of the Physical Sciences, 2011, 6(15), pp. 3704-3710.